Letter

Buildup dynamics of room-temperature polariton condensation

Fei Chen,[1] Hang Zhou,[2] Ziyu Ye,[1] Song Luo,[2] Zheng Sun,[1] Yuanlin Zheng,[3] Xianfeng Chen,[3,4] Huailiang Xu,[1] Hongxing Xu,[1] Tim Byrnes,[5,1,6,7,8] Hui Li,[1,*] Zhanghai Chen,[2,11,12,†] and Jian Wu[1,9,10,‡]

[1]*State Key Laboratory of Precision Spectroscopy, East China Normal University, Shanghai 200241, China*

[2]*Department of Physics, College of Physical Science and Technology, Xiamen University, Xiamen 361005, China*

[3]*State Key Laboratory of Advanced Optical Communication Systems and Networks, School of Physics and Astronomy, Shanghai Jiao Tong University, Shanghai 200240, China*

[4]*Collaborative Innovation Center of Light Manipulation and Applications, Shandong Normal University, Jinan 250358, China*

[5]*Division of Arts and Sciences, New York University Shanghai, 1555 Century Ave, Pudong New District, Shanghai 200122, China*

[6]*NYU-ECNU Institute of Physics at NYU Shanghai, 3663 Zhongshan Road North, Shanghai 200062, China*

[7]*Department of Physics, New York University, New York, New York 10003, USA*

[8]*Center for Quantum and Topological Systems (CQTS), NYUAD Research Institute, New York University Abu Dhabi, United Arab Emirates*

[9]*Collaborative Innovation Center of Extreme Optics, Shanxi University, Taiyuan, Shanxi 030006, China*

[10]*CAS Center for Excellence in Ultra-intense Laser Science, Shanghai 201800, China*

[11]*Wuhan National High Magnetic Field Center, Wuhan 430074, China*

[12]*Collaborative Innovation Center of Advanced Microstructures, Nanjing University, Nanjing, Jiangsu 210093, China*

(Received 2 May 2022; revised 30 June 2022; accepted 7 July 2022; published 19 July 2022)

By using the femtosecond angle-resolved spectroscopic imaging technique, the ultrafast buildup dynamics of room-temperature polariton condensation is explicitly visualized in a ZnO whispering gallery mode microcavity. The buildup time of polariton condensation with respect to the arrival of the femtosecond pump pulse decreases with the increasing pump power and reaches a lower limit of about 4 ps. Simulation results by numerically solving the open-dissipative Gross-Pitaevskii equation coupled to an incoherent reservoir are in quantitative agreement with the experimental observations, showing that the scattering from exciton reservoir to the lower polariton branches and the decay from these branches dominate the buildup process.

DOI: 10.1103/PhysRevB.106.L020301

Exciton polaritons (EPs), which are hybrid quasiparticles formed by the strong coupling between excitons and confined microcavity photons [1,2], have attracted much attention in recent years due to their rich physics and diverse potential applications. The bosonic nature of these quasiparticles makes them an ideal testing ground for the study of macroscopic quantum phenomena. When the interparticle distance decreases to the level of their de Broglie wavelengths [3], EPs can accumulate massively in a single quantum state, and can occur at high temperatures due to the extremely light effective mass, forming a driven dissipative Bose-Einstein condensate (BEC). A BEC of EPs has been realized in two-dimensional (2D) quantum wells at cryogenic temperatures [4,5], attracting considerable attention due to possessing quantum properties at the macroscopic level, such as superfluidity [6], vortex formation [7], soliton propagations [8], etc. Moreover, the excitonic component gives EPs rich nonlinear effects. This makes EPs a good candidate to realize several key quantum devices [9], such as polaritonic parametric amplifier [10,11], polariton transistor switch [12], and logic gates [13–15].

While fundamental to the understanding of the underlying mechanism of condensation in such devices, the exact mechanism of the ultrafast buildup of condensation and evolution of coherence has never been measured in a room-temperature microcavity polariton condensate. In these cases, the energy exchange of the quasiparticles with the lattice becomes stronger, thus the dissipation of polaritons is significantly accelerated compared to lower temperatures samples [16]. The dynamics of polaritonic condensation at cryogenic temperatures has been recorded with pisosecond resultion in GaAs and CdTe microcavities, utilizing a streak camera [17,18]. In contrast, the formation of a BEC at room temperature requires subpicosecond resolution, which is not accessible by using commercial streak cameras. Nevertheless, a variety of time-resolved schemes have been developed for the detection of ultrafast polaritonic dynamics. For instance, off-axis digital holography has been introduced to acquire both the amplitude and phase information of the EP wave packets in real space [19]. Femtosecond angle-resolved spectroscopic imaging (FARSI) technique has been developed to explore the femtosecond dynamics of polariton bosonic cascading effect and polariton parametric scattering [20,21].

Here, utilizing the FARSI technique in combination with nonresonant femtosecond excitation, the angle-resolved ultrafast buildup and relaxation dynamics of EP condensates have been investigated with subpicosecond time resolution

*hli@lps.ecnu.edu.cn
†zhanghai@xmu.edu.cn
‡jwu@phy.ecnu.edu.cn

in a ZnO whispering gallery mode (WGM) microcavity at room temperature. It is demonstrated that the buildup time of room-temperature polariton condensation is of the order of a few picoseconds. The measured buildup dynamics of the population of EP condensates can be well reproduced using an open-dissipative Gross-Pitaevskii (GP) equation coupled to an incoherent reservoir, indicating that the scattering of the reservoir excitons towards the lower polariton (LP) branches in combination with the relaxation of these LP branches plays a dominant role in the buildup of polariton condensation. A better understanding of the underlying mechanism of condensation can provide the foundation for ultrafast and precision manipulation of polariton condensates towards the development of advanced devices.

We first briefly summarize our experimental configuration. The ZnO microwire was grown along the c axis by carbothermal reduction on a (111) silicon substrate at 1100 °C [22]. The hexagonal cross section structure forms a natural WGM microcavity which possesses a high quality factor (Q factor) of around 1000 [23,24]. Due to its large exciton binding energy (around 60 meV) and strong oscillator strength, the ZnO microcavity provides an excellent platform to study exciton polariton condensation in the strong coupling regime at room temperature [25–30]. The pump laser pulses at the central wavelength of about 350 nm were generated by frequency conversion from the output of a Ti:sapphire amplification system (35 fs at 800 nm, 1 kHz) through an optical parametric amplifier. The duration of these pump pulses is about 70 fs. The ZnO microwire was excited nonresonantly through a 15× objective with a numerical aperture of NA = 0.15. The excitation spot size was ~3 μm in diameter. The FARSI technique was applied to measure the dynamics of polariton condensation with femtosecond time resolution [20,21,31]. In this technique, a transient optical Kerr gating was implemented in the angle-resolved spectroscopic imaging in the Fourier space, providing time-resolved visualization of the photoluminescence (PL) distribution from the ZnO microwire in both the energy and the momentum degrees of freedom. The PL signal was finally recorded by an Andor spectrometer (with the focal length of 500 mm and the grating specific as 1200 g/mm) with an intensified charge-coupled device camera. Intense femtosecond laser pulses at 800 nm obtained directly from the Ti:sapphire amplification system (noted as the gating pulses) introduce transient birefringence in the Kerr medium, realizing an ultrafast shutter along the light path of the PL. The arrival time of the gating pulses is controlled by a high-precision motorized stage. Importantly, the optical dispersion induced by all related optical elements was characterized by performing a comparison measurement [20]. The absolute zero time point (defined as the instant that the pump laser pulse arrives at the ZnO sample) can be well determined, which is one of the key issues to unambiguously measure the buildup and relaxation dynamics of the polariton condensation with femtosecond precision.

The angle-resolved PL emissions below and above the condensation threshold obtained from the ZnO WGM microcavity are shown in Figs. 1(a) and 1(b). Figure 1(a) shows the typical dispersion mapping with multiple LP branches obtained in a ZnO microwire in the linear regime (the dashed white lines are the fitting results obtained from the plane

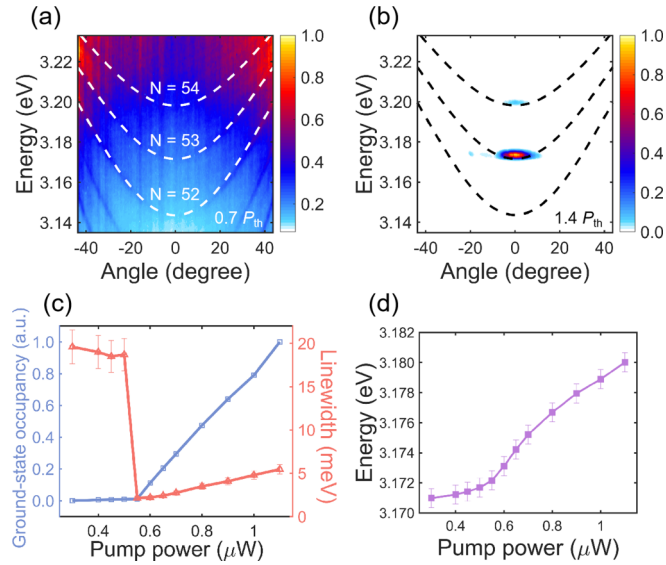

FIG. 1. Photoluminescence distributions as a function of emission angle and energy obtained for the k-space measurement at a pump power (a) below and (b) above the condensation threshold, respectively. Pump power dependence of (c) the ground-state occupancy, the spectral linewidth, and (d) the energy at the maximum of the PL emission spectra.

wave model [32]). When the pump power is increased from 0.4 to 0.78 μW, clear signatures for polariton condensation concentrating around $k_{\parallel} = 0$ ($k_{\parallel}$ represents the momentum in the direction parallel to the microwire) emerge as shown in Fig. 1(b). The polariton condensate is preferentially formed on an optimized WGM with the highest quality factor [33] (here is the LP mode with $N = 53$), determined by the media loss and the cavity loss. Figure 1(c) shows the pump power dependence of the ground state occupancy and the PL emission linewidth. The energy at the maximum of the PL emission spectra as a function of the pump power is shown in Fig. 1(d). A sharp increase in the ground-state occupation can be recognized above the pump threshold at about 0.55 μW (defined as P_{th} aftwards), where the linewidth narrows dramatically. An energy blueshift of the PL of about 10 meV can be observed. These signatures demonstrate the formation of a polariton condensate in the strong coupling regime [25–30].

As schematically illustrated in Fig. 2(a), the buildup process of polariton condensation can be described as follows. First, a transient exciton population (noted as hot exciton) above the band gap is created by the nonresonant excitation. These electron-hole pairs relax towards a lower energy reservoir, noted as reservoir excitons. When the reservoir exciton reaches sufficiently high density, the scattering rate of the excitons to the LP branch overruns its losses, forming exciton polaritons. Later, the polaritons on the LP branches slide towards the ground state via relaxation pathways of, e.g., interaction with optical phonons and polariton-polariton scattering [4]. When the occupation of the ground state is above a certain threshold, polaritons accumulate massively and the BEC is realized. Here, we divide the whole process of polariton condensation into three steps [4,34,35]. Step 1: hot excitons are created through excitation of the pump pulses,

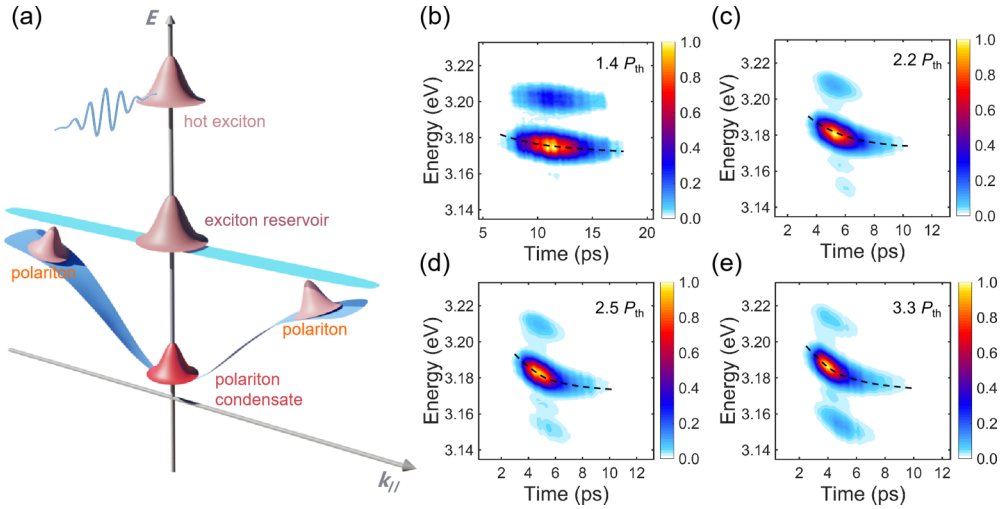

FIG. 2. The dynamics of polariton condensation at different pump powers. (a) A schematic drawing of the buildup dynamics during polariton condensation. (b)–(e) The angle-integrated PL distribution as a function of time and energy at the pump powers of $1.4P_{\text{th}}$, $2.2P_{\text{th}}$, $2.5P_{\text{th}}$, and $3.3P_{\text{th}}$, respectively. The black dashed curves are to guide the eye to indicate the redshift during polariton condensation relaxation.

and trickle down in energy to the reservoir exciton level. This "trickle down" process is very fast with negligible time. Step 2: the reservoir excitons, especially locating at large k, are strongly coupled with the cavity mode, generating exciton polaritons. Step 3: polaritons relax along the LP branch and form BEC when a high pump power above the condensation threshold is applied.

In this work, the femtoseond-resolved dynamics of the EP condensation are unambiguously visualized by the FARSI technique. As shown in Figs. 2(b)–2(e), the angle-integrated PL distributions of the polariton condensate as a function of the emission energy and time exhibit distinct pump power dependent features. At these pump powers, polariton condensates beyond that of a single LP branch can be obtained. As the pump power increases, a larger number of polaritons accumulate on the ground state, accompanied with stronger interaction among the quasiparticles. This results in the broadening of the polariton mode, originating from the repulsive interactions between the exciton components [36], with an observable initial blueshift. Since there are no additional supplements after the accomplishment of the femtosecond pump pulse, the condensate emission decays with a redshift caused by a continuous reduction of the total carriers [18,20] [indicated by the black dashed curves in Figs. 2(b)–2(e)].

By integrating the signals from all the LP branches in the energy domain, the polariton population as a function of time can be obtained for various pumping strengths and are explicitly shown in Fig. 3(a). The arrival time of the maximum population of the polaritons with respect to the pump laser pulse, corresponding to the buildup time, and the full width at half maximum (FWHM) of the time-dependent PL strength for different pump powers are shown in Fig. 3(c). We can see that the stronger pump pulse leads to faster dynamics, manifested in both the buildup and the decay processes, which is consistent with polaritonic dynamics on a time scale of tens of picoseconds under cryogenic temperatures [37]. We observe that the particle density plays a crucial role. The acceleration of the bulidup process can be attributed to the increased collision rate among excitons with strong pumping. Benefiting from the FARSI technique, the zero time can be explicitly determined in our work, and thus the buildup time of the polariton condensation can be obtained here with femtosecond precision. Nevertheless, the coherence may need extra time to be established due to the certain speed for formation of the coherent phase in a polariton condensate, resulting in a delayed long-range order compared to the buildup of the EP population [37]. Here, we find that the buildup time decreases with the pumping power and reaches a lower limit when the

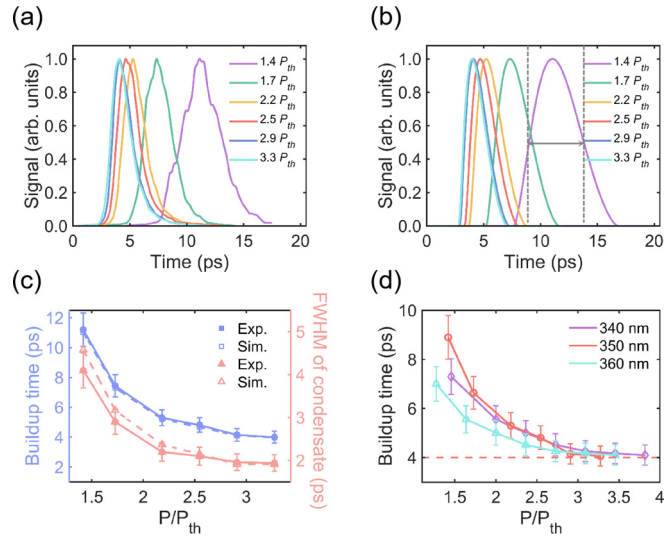

FIG. 3. The time-dependent population of the polariton condensate for various pump powers obtained from (a) experimental measurements and from (b) numerical simulations. The population are comprised of the signals from all the LP branches. (c) Pump power dependence of the buildup time and the FWHM [indicated by the grey dotted lines in (b)] of the polariton condensate. (d) Pump power dependence of the buildup time of polariton condensation obtained at different excitation wavelengths. The corresponding condensation thresholds are 0.58 μW (340 nm), 0.55 μW (350 nm), and 0.57 μW (360 nm), respectively.

power is increased beyond about $3P_{\text{th}}$. The shortest "buildup time" of the polarition condensation is observed to be about 4 ps.

The buildup and relaxation dynamics can be quantitatively reproduced by numerically solving an open-dissipative Gross-Pitaevskii (GP) equation coupled to an incoherent reservoir. In this model, we consider the LP mode amplitude ψ to be coupled to an incoherent reservoir density n_{R} [38,39]. The equations are written as follows:

$$\frac{\partial n_R(x,t)}{\partial t} = P(x,t) + Rn_R(x,t)|\psi(x,t)|^2 - \gamma_R n_R(x,t), \quad (1)$$

$$i\frac{\partial \psi(x,t)}{\partial t} = -\frac{\hbar}{2m}\nabla^2\psi(x,t) + g_R n_R(x,t)\psi(x,t) + g_C|\psi(x,t)|^2 + i(Rn_R(x,t) - \gamma_C)\psi(x,t). \quad (2)$$

Here, $P(x, t)$ is the pump in real space, ψ represents the polariton wave function, n_{R} and γ_{R} represent the density and the decay rate of the reservoir excitons, and R is the scattering rate from the exciton reservoir to the LP branch. By setting a proper detection efficiency on the calculated results (in analogy to the detection threshold of the experiments), the observed dynamics can be well reproduced, as shown in Figs. 3(b) and 3(c). A polariton lifetime of about 2.3 ps can be obtained from the simulation. We may see in Fig. 3(c) that the derived buildup times agree well with the calculated results and the measured data. These results show that the buildup time possesses a lower limitation when the excited exciton density reaches a certain level. We may see from the simulation that the combined influence of the scattering rate from the exciton reservoir towards a certain LP branch and the decay rate of this branch determine the eventual buildup dynamics. A stronger scattering and a faster decay result in a shorter buildup time. We expect that the limitation of the condensate buildup time is dependent on the cavity quality. Meanwhile, we note that the observed ultrafast polariton condensation signal can be regarded as a polariton lasing with a duration of a few picoseconds [20]. The pump power dependence of the FWHM of the lasing signal is extracted and is plotted in Fig. 3(c). As the pump power increases, the value of FWHM decreases from 4.2 to 1.9 ps, showing a similar saturation tendency compared to that of the buildup time. This indicates that the pulse duration of the polariton lasing can be tailored by tuning the strength of the pump pulses.

Pump laser pulses with different excitation wavelengths are applied to check the influence of step 1 on the buildup process. The initially formed hot excitons on different energy levels may take different time trickling down to the exiton reservoir. As shown in Fig. 3(d), the pump power dependent buildup time shows similar trends and converges at the same lower limit of about 4 ps. This means that the hot excitons formed on various energy levels do not show an explicit difference on the limitation of the buildup time of the polariton condensation. Therefore we believe that the time consumed by step 1 could be extremely short, which is not detectable in the present work. The time that the hot excitons scattered to reservoir excitons can be ignored;we consider that this is a reasonable approximation in the context of modelling the

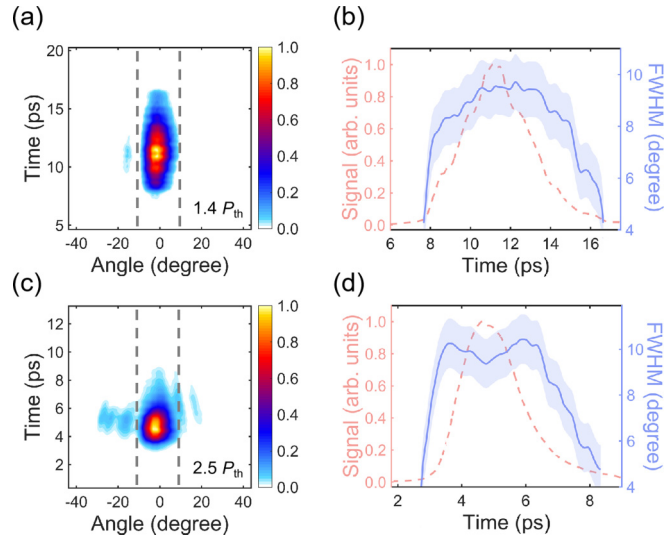

FIG. 4. Time-resolved population and momentum distribution of the polariton condensate. (a) The PL distribution as a function of time and angle obtained for the k-space measurement at a pump power of $1.4P_{\text{th}}$. (b) The derived time-dependent population (the red dashed curve) and the FWHM (the blue curve) in the region of $(-10°, +10°)$ obtained from (a). Panels (c) and (d) are similar to those of (a) and (b) but for a pump power of $2.5P_{\text{th}}$.

polariton condensation. The buildup time is dominated by the time consumed by steps 2 and 3. The deviation at the excitation wavelength of 360 nm may be related to the fact that 360 nm locates on the sideband of the absorption spectrum of ZnO microwire. This may cause a different amount of excitation in the instantaneous particle density thus affecting the following buildup dynamics.

Time-resolved angular distribution of the PL can be also obtained using the FARSI technique. Figures 4(a) and 4(c) show the PL distributions as a function of time and angle in the k space, under two distinct pump powers, i.e., $1.4P_{\text{th}}$ and $2.5P_{\text{th}}$. The time-resolved FWHM of the momentum distributions are extracted for the angle range between $-10°$ and $+10°$ and are shown in Figs. 4(b) and 4(d) (blue lines). An apparent shrinking of the angular distribution can be observed at the moment of the maximum EP population at the pump power of $2.5P_{\text{th}}$. The polariton condensation evolves with two correlated processes, i.e., the dynamics of polariton distribution and the establishment of spatial coherence [40]. For the excitation power slightly exceeding the condensation threshold (at $1.4P_{\text{th}}$), both the density and the width of the momentum distribution show an increasing and later decreasing trend as a function of time, as shown in Fig. 4(b). Under a stronger pump power (at $2.5P_{\text{th}}$), a large number of polaritons occupy the ground state of a certain lower polariton branch, accelerating the formation of coherence. When the occupation increases to a certain level, the fast establishment of coherence can be induced due to stronger interaction among polaritons, which will result in a narrowing in the k-space distribution. This can be found in the derived results shown in Fig. 4(d). The absorption of the excitation photons does not exhibit a saturation effect in the explored conditions, thus the narrowing of the polaritonic angular

distribution cannot be induced by the saturable absorption. The measurement of k-space angular distribution may serve as an extra criterion for the coherence property of polariton condensation.

In summary, based on the FARSI technique, the ultrafast buildup and relaxation dynamics of room-temperature polariton condensate have been visualized in a ZnO WGM microcavity with femtosecond precision. We have verified that the buildup time of polariton condensate decreases with pump strength and reaches a lower limit of about 4 ps in the present configuration. A narrowing of the angular distribution of the PL emission can be obtained approaching the end of the buildup process of BEC at higher pump power when a high degree of coherence can be established. Experimental results can be well reproduced by a model based on the open-dissipative Gross-Pitaevskii equation. Our results show that the buildup time is dominated by the process after the reservoir exciton is produced. The FARSI technique allows for direct observation of polariton condensation dynamics, which is very often simply assumed and not directly measured. Our work allows for the possibility of quantitative modeling and engineering of a very fundamental process in condensate formation, which should be beneficial towards future basic studies and potential applications of polariton systems.

This work was supported by the National Key R&D Program of China (Grants No. 2018YFA0306303 and 2018YFA0306304); the National Natural Science Fundation of China (Grants No. 92050105, No. 91950201, No. 11834004, and No. 12174111); and the project supported by the Science and Technology Commission of Shanghai Municipality, China (Grant No. 22ZR1419700). Z.C. acknowledges the support from the Fundamental Research Funds for the Central Universities (Grant No. 20720200074) and the Interdisciplinary Program of Wuhan National High Magnetic Field Center (Grant No. WHMFC202111). T.B. was supported by the National Natural Science Foundation of China (Grant No. 62071301); NYU-ECNU Institute of Physics at NYU Shanghai; the Joint Physics Research Institute Challenge Grant; the Science and Technology Commission of Shanghai Municipality (Grants No. 19XD1423000 and No. 22ZR1444600); the NYU Shanghai Boost Fund; the China Foreign Experts Program (Grant No. G2021013002L); and the NYU Shanghai Major-Grants Seed Fund. Z.S. acknowledges the support from Shanghai Pujiang Program Grant No. 21PJ1403000. F.C. acknowledges the support from the Fundamental Research Funds for the Central Universities (Grant No. YBNLTS2022-007).

[1] A. V. Kavokin and G. Malpuech, *Cavity Polaritons* (Elsevier, Amsterdam, 2003).
[2] J. J. Hopfield, Phys. Rev. **112**, 1555 (1958).
[3] T. Byrnes, N. Y. Kim, and Y. Yamamoto, Nat. Phys. **10**, 803 (2014).
[4] J. Kasprzak, M. Richard, S. Kundermann, A. Baas, P. Jeambrun, J. M. J. Keeling, F. M. Marchetti, M. H. Szymanska, R. Andre, J. L. Staehli, V. Savona, P. B. Littlewood, B. Deveaud, and L. S. Dang, Nature (London) **443**, 409 (2006).
[5] R. Balili, V. Hartwell, D. Snoke, L. Pfeiffer, and K. West, Science **316**, 1007 (2007).
[6] A. Amo, D. Sanvitto, F. P. Laussy, D. Ballarini, E. del Valle, M. D. Martin, A. Lemaitre, J. Bloch, D. N. Krizhanovskii, M. S. Skolnick, C. Tejedor, and L. Vina, Nature (London) **457**, 291 (2009).
[7] K. G. Lagoudakis, M. Wouters, M. Richard, A. Baas, I. Carusotto, R. Andre, L. Dang, and B. Deveaud-Pledran, Nat. Phys. **4**, 706 (2008).
[8] A. Amo, S. Pigeon, D. Sanvitto, V. G. Sala, R. Hivet, I. Carusotto, F. Pisanello, G. Lemenager, R. Houdre, E. Giacobino, C. Ciuti, and A. Bramati, Science **332**, 1167 (2011).
[9] D. Sanvitto and S. Kena-Cohen, Nat. Mater. **15**, 1061 (2016).
[10] M. Saba, C. Ciuti, J. Bloch, V. Thierry-Mieg, R. Andre, L. S. Dang, S. Kundermann, A. Mura, G. Bongiovanni, J. L. Staehli, and B. Deveaud, Nature (London) **414**, 731 (2001).
[11] P. G. Savvidis, J. J. Baumberg, R. M. Stevenson, M. S. Skolnick, D. M. Whittaker, and J. S. Roberts, Phys. Rev. Lett. **84**, 1547 (2000).
[12] T. Gao, P. S. Eldridge, T. C. H. Liew, S. I. Tsintzos, G. Stavrinidis, G. Deligeorgis, Z. Hatzopoulos, and P. G. Savvidis, Phys. Rev. B **85**, 235102 (2012).
[13] D. Ballarini, M. De Giorgi, E. Cancellieri, R. Houdre, E. Giacobino, R. Cingolani, A. Bramati, G. Gigli, and D. Sanvitto, Nat. Commun. **4**, 1778 (2013).
[14] A. V. Zasedatelev, A. V. Baranikov, D. Urbonas, F. Scafirimuto, U. Scherf, T. Stoferle, R. F. Mahrt, and P. G. Lagoudakis, Nat. Photon. **13**, 378 (2019).
[15] A. Dreismann, H. Ohadi, Y. d. V.-I. Redondo, R. Balili, Y. G. Rubo, S. I. Tsintzos, G. Deligeorgis, Z. Hatzopoulos, P. G. Savvidis, and J. J. Baumberg, Nat. Mater. **15**, 1074 (2016).
[16] D. Xu, W. Xie, W. H. Liu, J. Wang, L. Zhang, Y. L. Wang, S. F. Zhang, L. X. Sun, X. C. Shen, and Z. H. Chen, Appl. Phys. Lett. **104**, 082101(2014).
[17] E. del Valle, D. Sanvitto, A. Amo, F. P. Laussy, R. Andre, C. Tejedor, and L. Vina, Phys. Rev. Lett. **103**, 096404 (2009).
[18] M. De Giorgi, D. Ballarini, P. Cazzato, G. Deligeorgis, S. I. Tsintzos, Z. Hatzopoulos, P. G. Savvidis, G. Gigli, F. P. Laussy, and D. Sanvitto, Phys. Rev. Lett. **112**, 113602 (2014).
[19] L. Dominici, M. Petrov, M. Matuszewski, D. Ballarini, M. De Giorgi, D. Colas, E. Cancellieri, B. S. Fernandez, A. Bramati, G. Gigli, A. Kavokin, F. Laussy, and D. Sanvitto, Nat. Commun. **6**, 8993 (2015).
[20] F. Chen, H. Zhou, H. Li, J. H. Cao, S. Luo, Z. Sun, Z. Zhang, Z. Q. Shao, F. H. Sun, B. E. Zhou, H. X. Dong, H. L. Xu, H. X. Xu, A. Kavokin, Z. H. Chen, and J. Wu, Nano Lett. **22**, 2023 (2022).
[21] F. Chen, H. Li, H. Zhou, Z. Y. Ye, S. Luo, Z. Sun, F. H. Sun, J. W. Wang, H. L. Xu, H. X. Xu, Z. H. Chen, and J. Wu, J. Phys.: Condens. Matter **34**, 024001 (2022).
[22] S. Luo, Y. F. Wang, L. M. Liao, Z. Zhang, X. C. Shen, and Z. H. Chen, J. Appl. Phys. **127**, 025702(2020).
[23] M. Lorenz, A. Rahm, B. Q. Cao, J. Zuniga-Perez, E. M. Kaidashev, N. Zhakarov, G. Wagner, T. Nobis, C. Czekalla,

G. Zimmermann, and M. Grundmann, Phys. Status Solidi B **247**, 1265 (2010).
[24] C. Czekalla, T. Nobis, A. Rahm, B. Q. Cao, J. Zuniga-Perez, C. Sturm, R. Schmidt-Grund, M. Lorenz, and M. Grundmann, Phys. Status Solidi B **247**, 1282 (2010).
[25] L. Sun, Z. Chen, Q. Ren, K. Yu, L. Bai, W. Zhou, H. Xiong, Z. Q. Zhu, and X. Shen, Phys. Rev. Lett. **100**, 156403 (2008).
[26] A. Trichet, L. Sun, G. Pavlovic, N. A. Gippius, G. Malpuech, W. Xie, Z. Chen, M. Richard, and L. S. Dang, Phys. Rev. B **83**, 041302(R) (2011).
[27] W. H. Liu, D. Xu, W. Xie, H. X. Dong, J. Lu, S. F. Zhang, X. C. Shen, and Z. H. Chen, Appl. Phys. Express **6**, 091101 (2013).
[28] R. Schmidt-Grund, H. Hilmer, A. Hinkel, C. Sturm, B. Rheinlander, V. Gottschalch, M. Lange, J. Zuniga-Perez, and M. Grundmann, Phys. Status Solidi B **247**, 1351 (2010).
[29] T. Michalsky, M. Wille, M. Grundmann, and R. Schmidt-Grund, Nano Lett. **18**, 6820 (2018).
[30] F. Li, L. Orosz, O. Kamoun, S. Bouchoule, C. Brimont, P. Disseix, T. Guillet, X. Lafosse, M. Leroux, J. Leymarie, M. Mexis, M. Mihailovic, G. Patriarche, F. Reveret, D. Solnyshkov, J. Zuniga-Perez, and G. Malpuech, Phys. Rev. Lett. **110**, 196406 (2013).
[31] Z. Y. Ye, F. Chen, H. Zhou, S. Luo, F. H. Sun, Z. Sun, Y. L. Zheng, X. F. Chen, H. L. Xu, Z. H. Chen, H. Li, and J. Wu, J. Phys.: Condens. Matter **34**, 22LT01 (2022).
[32] T. Nobis, E. M. Kaidashev, A. Rahm, M. Lorenz, and M. Grundmann, Phys. Rev. Lett. **93**, 103903 (2004).
[33] T. Hu, W. Xie, L. Wu, Y. F. Wang, L. Zhang, and Z. H. Chen, Solid State Commun. **262**, 7 (2017).
[34] A. Askitopoulos, H. Ohadi, A. V. Kavokin, Z. Hatzopoulos, P. G. Savvidis, and P. G. Lagoudakis, Phys. Rev. B **88**, 041308(R) (2013).
[35] A. Kavokin, T. C. H. Liew, C. Schneider, and S. Hofling, Low Temp. Phys. **42**, 323 (2016).
[36] R. Su, C. Diederichs, J. Wang, T. C. H. Liew, J. X. Zhao, S. Liu, W. G. Xu, Z. H. Chen, and Q. H. Xiong, Nano Lett. **17**, 3982 (2017).
[37] G. Nardin, K. G. Lagoudakis, M. Wouters, M. Richard, A. Baas, R. André, L. S. Dang, B. Pietka, and B. Deveaud-Plédran, Phys. Rev. Lett. **103**, 256402 (2009).
[38] M. Wouters and I. Carusotto, Phys. Rev. Lett. **99**, 140402 (2007).
[39] T. Byrnes, T. Horikiri, N. Ishida, M. Fraser, and Y. Yamamoto, Phys. Rev. B **85**, 075130 (2012).
[40] D. A. Mylnikov, V. V. Belykh, N. N. Sibeldin, V. D. Kulakovskii, C. Schneider, S. Hofling, M. Kamp, and A. Forchel, JETP Lett. **101**, 513 (2015).